Inhibitory surrounds of motion mechanisms revealed by continuous tracking

Akshatha Bhat

IRCCS Stella Maris, Calambrone, Italy
Department of Neuroscience, University of Florence, Florence, Italy
✉

Guido Marco Cicchini

CNR Institute of Neuroscience, Pisa, Italy
✉

David C. Burr

Department of Neuroscience, University of Florence, Florence, Italy
CNR Institute of Neuroscience, Pisa, Italy
School of Psychology, University of Sydney, Sydney, Australia
✉

Continuous psychophysics is a newly developed technique that allows rapid estimation of visual thresholds by asking subjects to track a moving object, then deriving the integration window underlying tracking behavior (Bonnen, Burge, Yates, Pillow, & Cormack, 2015). Leveraging the continuous flow of stimuli and responses, continuous psychophysics allows for estimation of psychophysical thresholds in as little as 1 min. To date this technique has been applied only to tracking visual objects, where it has been used to measure localization thresholds. Here we adapt the technique to visual motion discrimination, by displaying a drifting grating that changes direction on a binary random walk and asking participants to continuously report drift direction by alternate key press. This technique replicates and confirms well-known findings of the motion-perception system. It also proves particularly valuable in demonstrating induced motion, reinforcing evidence for the existence of antagonistic surround fields. At low contrasts, the surround summates with the center, rather than opposing it, again consistent with existing evidence on classical techniques. The user-friendliness and efficiency of the method may lend it to clinical and developmental work.

Introduction

Visual thresholds are typically measured by forced-choice techniques where observers are required to make binary decisions about the size, orientation, direction of motion, or other quality of single, brief stimulus presentations. Robust measurements of thresholds require tens to hundreds of similar trials for each data point, making for long and usually boring testing sessions. This is problematic when testing typical young adults and can be prohibitive when testing very young or very old people, or clinical populations.

Bonnen, Burge, Yates, Pillow, & Cormack (2015) recently introduced a novel technique designed to circumvent these limitations based on a simple intuition: If a subject can see a stimulus well enough to answer psychophysical questions about it, they should also be able to accurately point to its position. They therefore asked subjects to continually point to the position of a randomly moving target and correlated this continuous response with the target trajectory. They showed that the strength of the correlation successfully predicted psychophysical thresholds measured by traditional two-alternative forced-choice techniques. This shows that manual tracking can yield abundant data in a very short time, unlike existing classical forced-choice paradigms. So far, however, this technique has been applied only to object tracking and measurement of localization thresholds.

Here we apply the technique of continuous tracking to motion discrimination, with the particular goal of studying induced motion and center–surround antagonistic mechanisms. We show that this technique can replicate well-known findings of the motion-perception system, encouraging the use of continuous psychophysics for testing visual function. We then extend the

technique to reveal center–surround antagonism and its dependence on contrast.

Center–surround antagonism is well known in neurophysiology and psychophysics. Classically, surround suppression is defined as a decrease in number of spikes as stimulus size is increased. The phenomenon has been observed at almost all the stages in vision, from retina to extrastriate cortex (Hartline, 1940; Barlow, 1981; Allman, Miezin, & McGuinness, 1985). It is crucial for figure–ground segregation (Allman et al., 1985), feature detection (Wiesel & Hubel, 1965), and so on, and seems to be a general principle for perceptual systems. Center–surround suppression applies not only to luminance signals but to many higher order signals. For example, there is clear psychophysical evidence of center–surround suppression for contrast (Chubb, Sperling, & Solomon, 1989) and for motion (Churan, Khawaja, Tsui, & Pack, 2008; Tadin, Lappin, Gilroy, & Blake, 2003).

Tadin et al. (2003) designed a series of elegant experiments showing that thresholds for motion discrimination (measured by varying duration) increase as the stimulus area increases, pointing to suppression. Interestingly, the suppression occurred only at relatively high contrasts, giving way to spatial summation at low stimulus contrasts. In a follow-up study the same group employed reverse-correlation techniques to infer the directionality and temporal extent of the influence of surround on target motion, and confirmed the earlier observation of repulsive effects at high target contrasts and assimilative effects at lower contrasts (Tadin, 2006). Recent neurophysiology studies have demonstrated surround suppression in neurons of MT (Churan et al., 2008), suggesting that they may be the neural substrate of these effects. This surround suppression is most evident with brief presentation durations, around 40 ms.

To demonstrate surround suppression in humans it is necessary to show that responsiveness decreases with stimulus area. Typically this involves measuring thresholds, by varying a parameter known to affect performance. Because suppression behaves differently for low and high contrasts, contrast cannot be used as the performance measure, so researcher have measured the minimum duration necessary to perceive direction. But this is also not ideal, as the surround suppression also depends on duration.

In this study we test the effectiveness of the new continuous-tracking technique to study motion perception, particularly surround antagonism. We find the technique to be effective, replicating and extending previous studies with standard psychophysical techniques.

Methods

Participants

A total of 14 participants (eight women, six men; mean age = 23 years) were recruited for the experiments. Apart from authors AB and GMC, none were aware of the purposes of the experiments. All had normal or corrected-to-normal vision. All participated with informed consent.

Stimuli and apparatus

In Experiment 1 the target stimulus was a vertical grating 2° high (hard edge) drifting horizontally within a 3.3° Gaussian envelope (full width at half height) at constant speed (0.5°/s), with a 0.5 probability of direction changes every 16 ms. In Experiment 2, the target was a vertical grating 2° high (hard edge) within a 0.35° Gaussian envelope (full width at half height), flanked above and below by vertical gratings of the same size and contrast. The two flankers drifted together but independently of the central grating, also with 0.5 probability of direction changes every 16 ms. Gratings drifted at 3.75 Hz in all cases (i.e., in one frame the phase of the grating changed by 1/32 of the full period). This means that the speed was 3.75°/s when the stimulus had spatial frequency of 1 c/° and 0.47°/sec when the stimulus was at 8 c/°.

All stimuli were displayed on a calibrated LCD display (Cambridge Research Systems Display ++) running at 120 Hz and subtending 70°. Stimuli were created in MATLAB (MathWorks, Natick, MA) with the Psychophysics Toolbox (Brainard, 1997; Kleiner et al., 2007). Participants viewed the stimuli from 57 cm from the screen in all conditions.

Each trial started by displaying the target drifting for 2 s rightward and 2 s leftward, to give a clear sense of direction to the participant, and 2 s of pause. Then for 1 min the target drifted left and right, changing direction with probability 0.5 every 16 ms. Participants were asked to indicate the direction with left and right arrow keys, following as well as possible the instantaneous direction of the target. Tracking data were collected using the standard USB keyboard (tested to have a resolution of 4 ms). Subjects were instructed to press one key at a time. If during the transitions there was either no key press or pressure on both keys, we considered the last unique key press. Figure 1a and Supplementary Movie S1 give examples of the stimulus velocities and the response, and Figure 1b gives the corresponding series of subject response.
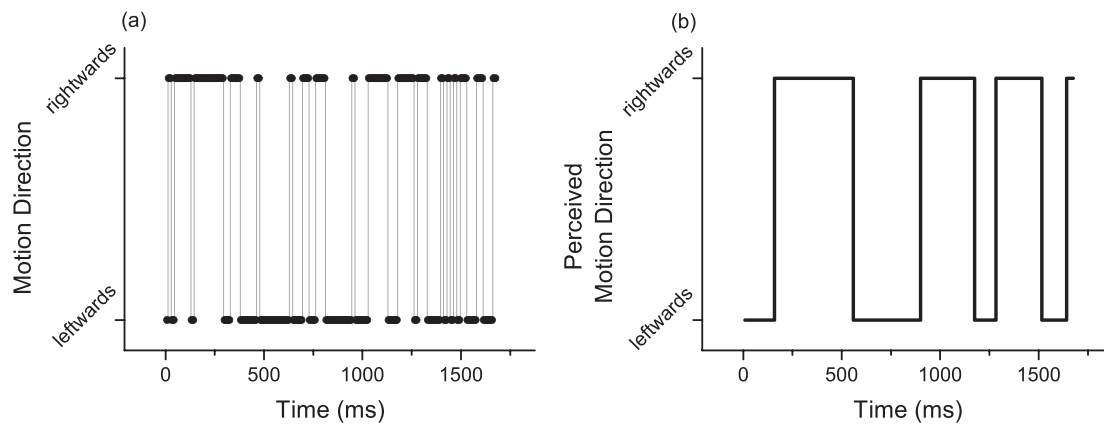
Figure 1. Sample stimulus drifting direction and response. (a) Example physical direction of drifting gratings of random direction, equiprobably left and right, changing direction with probability 0.5 every 16 ms. (b) Subject tracking response for the stimulus in (a). See also Supplementary Movie S1 for an illustration of stimulus (1 c/°, 8% Michelson contrast).

Procedure

Participants were asked to track the target grating drifting left and right randomly. Experiment 1 examined the effect of varying spatial frequency and contrast, using gratings of 1 and 8 c/° at 8% Michelson contrast or gratings of 1 c/° at six levels of contrast: 0.5%, 0.7%, 1%, 2%, 4%, and 8%. For each condition, four 1-min sessions were acquired.
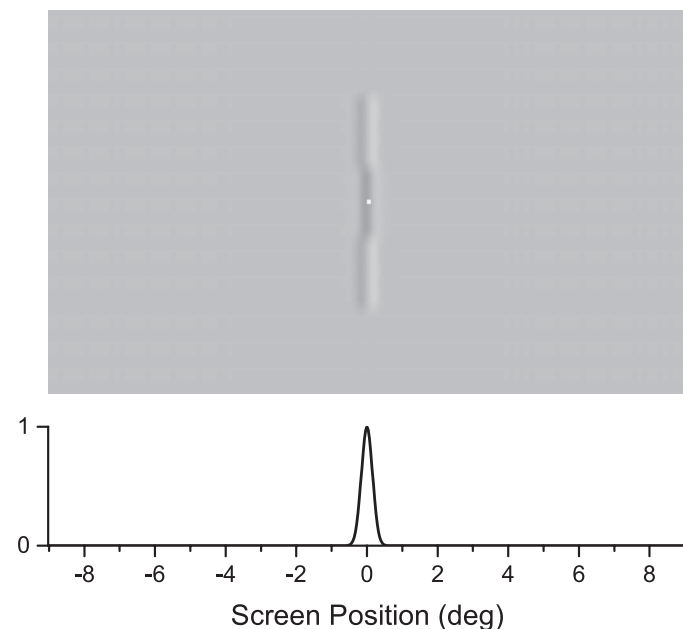

Figure 2. Example stimulus for Experiment 2. The target in the center is a Gaussian of 0.35° (full width at half height), flanked above and below by gratings of the same contrast and spatial frequency. Flankers also move left and right randomly, but independent of the target. Michelson contrast of the target and surround varied in each session from 1% to 16%.

In the second experiment, subjects were still required to track a central grating, but this time two flankers were present above and below the target (Figure 2). The flankers were presented within the same Gaussian envelope that vignetted the target grating. Flankers always had the same contrast as the target but drifted (together) randomly independent of target direction. Target and flanker Michelson contrasts varied from 1% to 16% in octave steps; for each contrast, three sessions were acquired.

Data analysis

For each subject and condition, we first pooled all the data by appending the various sessions, then calculated the cross-correlogram (CCG) between stimulus and response. As CCGs imply a continuous multiplication of a random stimulus and the subject response, they bear a strong similarity to reverse-correlation techniques. Indeed, each CCG is akin to an average kernel derived by reverse-correlation techniques (Ahumada, 1996; Neri & Levi, 2006)

Each CCG was then fitted with a Gaussian function, defined by its peak, lag, and width (along with 95% confidence bounds). Figure 3 shows example kernels from which CCGs for target and surround were obtained (see Supplementary File S2 for the goodness of fits).

Kernel parameter values (peak, lag, and width) as a function of contrast were fitted with a standard Naka–Rushton equation (Naka & Rushton, 1966):

$$y = A \frac{x^{\beta}}{x^{\beta} + C_{50}^{\beta}} + B$$

where C_{50} is the semisaturating contrast, A is the overall modulation, and B is the baseline. The value of A was constrained to reflect an improvement with
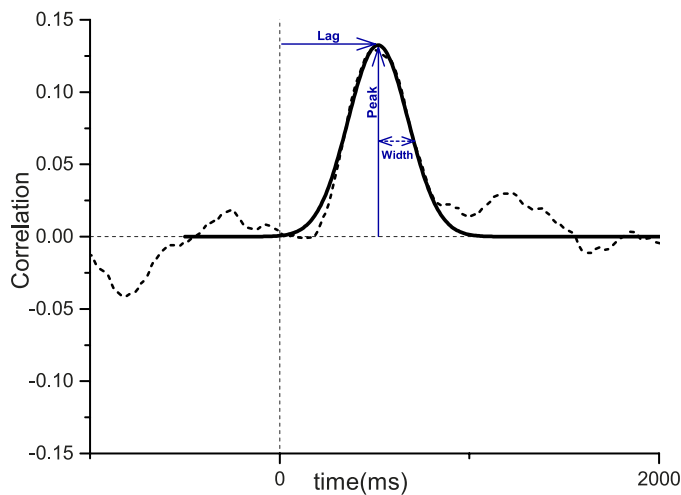
Figure 3. Example cross-correlogram for Experiment 1, at 16% contrast and 1 c/°. Cross-correlation values plotted against time for target (dashed line) and then fitted with Gaussian function (solid line) to obtain the parameters.
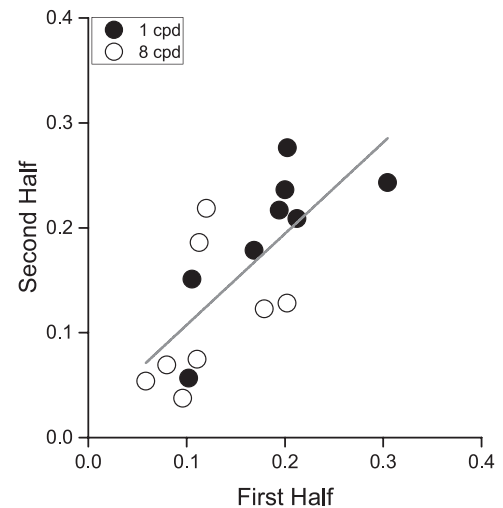

Figure 5. Reliability test for the peak of the Gaussian obtained across the trials for 1 and 8 c/°. Split-half analysis plotting peak correlation for the kernel obtained with the second half of the experimental data collection (three sessions) versus the peak correlation of the cross-correlogram from the first half of the data collection. Black points and hollow points refer to the 1 and 8 c/° cross-correlograms, respectively.

contrast, positive for the peak and negative for the width and lag. The parameter β determines the steepness of the sigmoidal function. In Experiment 1, Task 2, we measured CCGs at six contrasts, which allowed us to fit all four parameters of the Naka–Rushton equation including β, which was set to vary between 2 and 4. When fitting the kernels of Experiment 2, on the other hand, we had only five data points, so we decreased the free parameters to three. As β has generally little impact on the asymptote of the Naka–Rushton function, we fixed it to 3, close to the average value it took in the fits of Experiment 1, Task 2 (see caption of Figure 6).

Fitting procedures were carried out in MATLAB using the fit functions of the Curve Fitting toolboxes. By default, the objective function was linear least

squares and the fit algorithm was Trust-Region. No robust fitting algorithm was employed.

Results

Effect of spatial frequency and stimulus contrast on continuous tracking

Subjects were asked to continuously track the direction of drift of a moving grating by pressing the
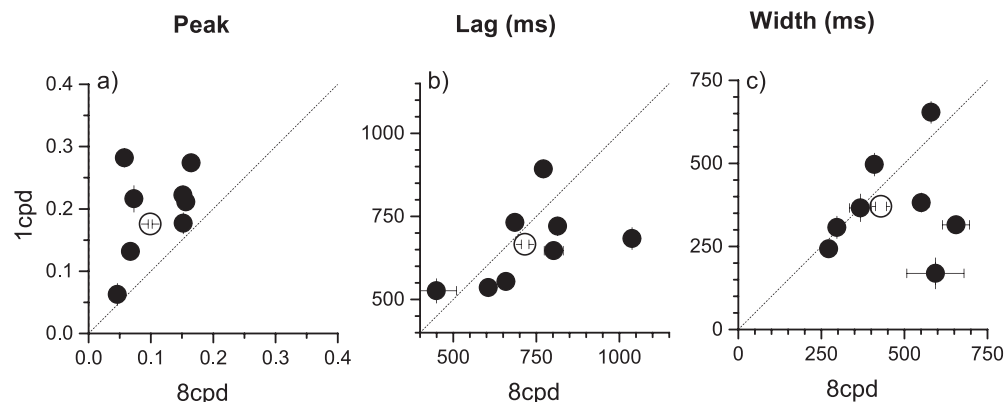

Figure 4. Parameters of the Gaussian cross-correlograms for 1 and 8 c/°. Peak (a), lag (b), and width (c) derived from the Gaussian fit to each subject's data for 8 c/° are plotted against the same parameters for 1 c/° (unfilled dots are the values for the aggregate subject; error bars correspond to the standard error of the mean; filled dots are individual data and error bar is 95% confidence interval returned by the fitting function; both gratings at 8% Michelson contrast).
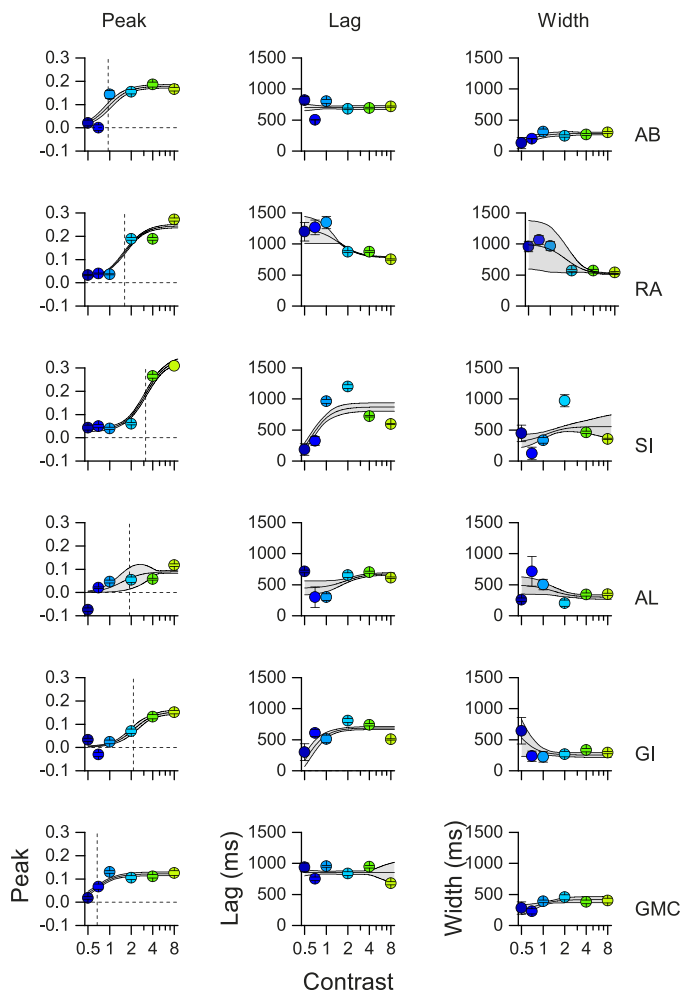
Figure 6. Kernel parameters as a function of target contrast for six subjects. Each column shows peak, lag, and width of the cross-correlograms. Error bars represent 95% confidence interval as returned by the Gaussian fit. Black lines and shaded area show best-fitting Naka–Rushton functions along with 95% confidence bands obtained via bootstrapping. Only in the case of peak do we obtain fitting parameters significantly different from zero; dashed vertical lines indicate C_{50} values; β was always between 2.8 and 3.1 (see Supplementary File S2 for all the fit parameters).

appropriate arrow key. The time series of this tracking was then related to the physical time series by cross-correlation (Mulligan, Stevenson, & Cormack, 2013). The resulting CCG plots the correlation between two vectors of time-series data as a function of lag between them. Figure 3 shows an example CCG for one participant. For each participant and each condition, we calculate the CCG and fit it with a Gaussian function free to vary in height, width, and lag.

We first tested continuous tracking for motion at 8% contrast, contrasting performance with gratings of 1 c/° (close to the optimum for motion perception) and 8 c/°, a much more challenging stimulus for the motion

system. For each spatial frequency we calculated the CCG and fitted it with a Gaussian, each with three parameters: peak, lag, and width. Figure 4 shows how these parameters varied with the two spatial frequencies, plotted separately. We expected that when motion-direction discrimination is easier (at 1 c/°), the correlation between stimulus and response trajectories should be stronger, resulting in a higher peak, lower latency (lag), or tighter kernels (or all three).

It is clear from Figure 4 that the peak amplitude of all subjects is higher at 1 than at 8 c/° (all points above the equality line). However, for lag and width there was no clear advantage. This was confirmed by paired-sample one-tailed t tests. The difference in peak scores was significant, $t(7) = 4.05$, $p = 0.004$, but those for lag and width were not—respectively, $t(7) = -1.37$, $p = 0.20$, and $t(7) = -1.57$, $p = 0.16$. Peak amplitude of the kernel seems to be the most robust parameter, varying with the visibility of drifting gratings.

As Bonnen et al. (2015) demonstrated, reliable tracking can be obtained even with sessions as short as a few minutes; we tested whether the binary motion-tracking paradigm also provides reliable estimates with short experimental sessions. To do so we employed a split-half reliability technique. For each subject and condition, we compared the first three experimental sessions with the last three. Figure 5 shows the CCG peak for the second half of the trials plotted against the first half. The two values tend to be very similar, resulting in a correlation coefficient of 0.72 ($p = 0.0014$), which is similar to many other psychophysical paradigms, including two-alternative forced-choice judgments (see Anobile, Castaldi, Turi, Tinelli, & Burr, 2016). Interestingly, this high value was obtained with sessions lasting only 3 min, indicating a good potential of the technique.

In a second task, we measured continuous tracking for motion at six different contrast levels between 0.5% and 8%, keeping spatial frequency at 1 c/°. Again, we expected all the parameters of the correlation to improve as the contrast increased.

As with spatial frequency, peak amplitude was found to be the most robust parameter to reflect performance improvement with contrast. Figure 6 plots peak, lag, and width of the kernel as a function of stimulus contrast. By inspection, it is clear that the peak is the only measure that displays a robust positive dependence on contrast. This was confirmed by fitting the various curves with a Naka–Rushton equation (see methods). The peak of the CCG gave an excellent fit (average R^2 of 0.83 ± 0.06), suggesting it is a good measure of the contrast dependence. The other two parameters, however, which are expected to decrease with contrast increases, did so only occasionally (2/6 times for lag and 3/6 for width), with much poorer fits
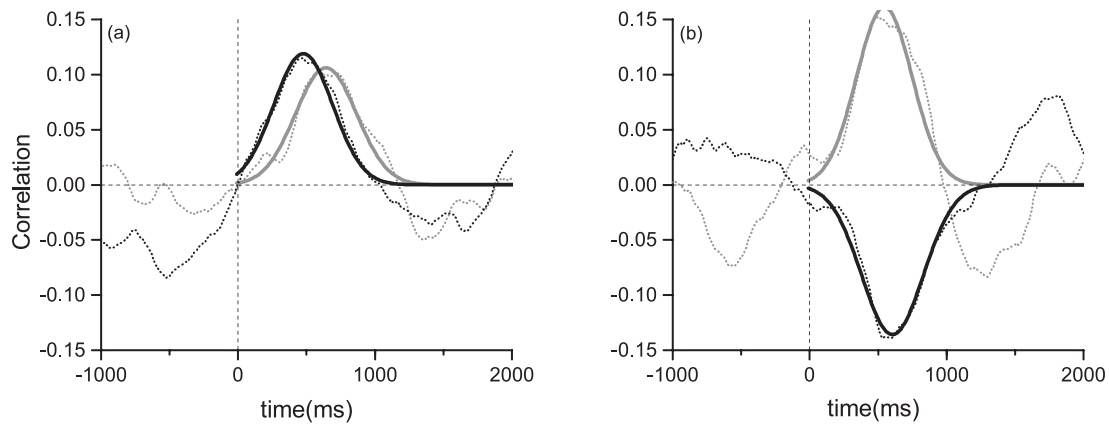
Figure 7. Example cross-correlogram for Experiment 2 at 2% and 16% contrast. Cross-correlation as a function of time for target (gray) and for surround (black). Cross-correlograms are indicated by thin dashed thin lines, best-fitting Gaussian functions by thick solid lines (data are from subject RA).

(average $R^2 = 0.21 \pm 0.16$ and 0.23 ± 0.17, respectively).

Effect of surround on continuous tracking

Having established that continuous tracking is a viable method to study human motion perception, we tested whether it could also reveal surround antagonistic effects. Here the moving target was surrounded by flanker gratings of the same contrast that moved independently of the target, at the same average speed. The independent random motion of the surround allows estimation of the influence of the surround on target tracking in different tracking conditions, by correlating the response with the motion trajectories of both the center and the surround (see Figure 2).

Sample CCGs are shown for two contrasts, 2% (Figure 7a) and 16% (Figure 7b). In this example, the CCGs between target motion and response are positive at both contrasts. Interestingly, the CCG between surround motion and response varies with contrast. At high contrasts it has a strong negative peak, implying motion antagonism. Although subjects were instructed to ignore the movement of the surrounds, these clearly affected the perceived motion of the central grating, which would seem to move in the opposite direction (giving a negative correlation). At low contrasts, on the other hand, the CCG is positive, implying that the subject response draws upon all motion signals presented, indicating spatial pooling of motion signals.

Figure 8a and 8b plots the peak of the CCGs between response and target and between response and surround for all subjects at all contrasts tested. The plots of Figure 8a replicate the results of Figure 6, showing that the peak of the CCGs monotonically grows with stimulus contrast. Transition points of the Naka–Rushton functions sit in the middle of the

contrasts tested, consistent with the choice of narrow stimuli, which have a higher threshold than those of Experiment 1.

Figure 8b reinforces the sample data shown in Figure 7 and shows how at low contrasts, CCGs between response and surround motion are positive, signaling motion integration of the surround with the target. At higher contrasts, CCGs are consistently negative, indicating motion antagonism.

Figure 8b also shows that the exact shape of the curves differs somewhat between subjects. Some subjects show a positive peak only at the lowest contrast (MCM and GI), while others show a positive peak for contrasts up to 4% (SI and GMC). At times the CCG at the lowest contrast is below threshold and then becomes positive as soon as threshold is exceeded (SI, RA). Given this intersubject variability, we attempted to summarize the different results for high and low contrasts from the asymptotes of the Naka–Rushton fit. The Naka–Rushton function has two asymptotes, one at low contrasts (B) and one at high contrasts (A). We used these asymptotic values to define high and low contrasts for the purpose of our comparison.

Figure 9 plots the values of these low and high contrast asymptotes for both the target and the surround CCGs, for individual participants (symbols) and for the group average. These results confirm the trends made apparent by inspection of Figure 8a and 8b. Importantly, at low contrasts the peaks were significantly higher than zero both for the target, $t(7) = 6.15$, $p = 0.0005$, and the surround, $t(7) = 7.34$, $p = 0.0002$, indicating spatial pooling. At high contrasts the target CCGs have a significantly positive peak, $t(7) = 3.99$, $p = 0.0053$, and the surround CCGs have a significantly negative peak, $t(7) = -5.70$, $p = 0.0007$, indicating motion antagonism.
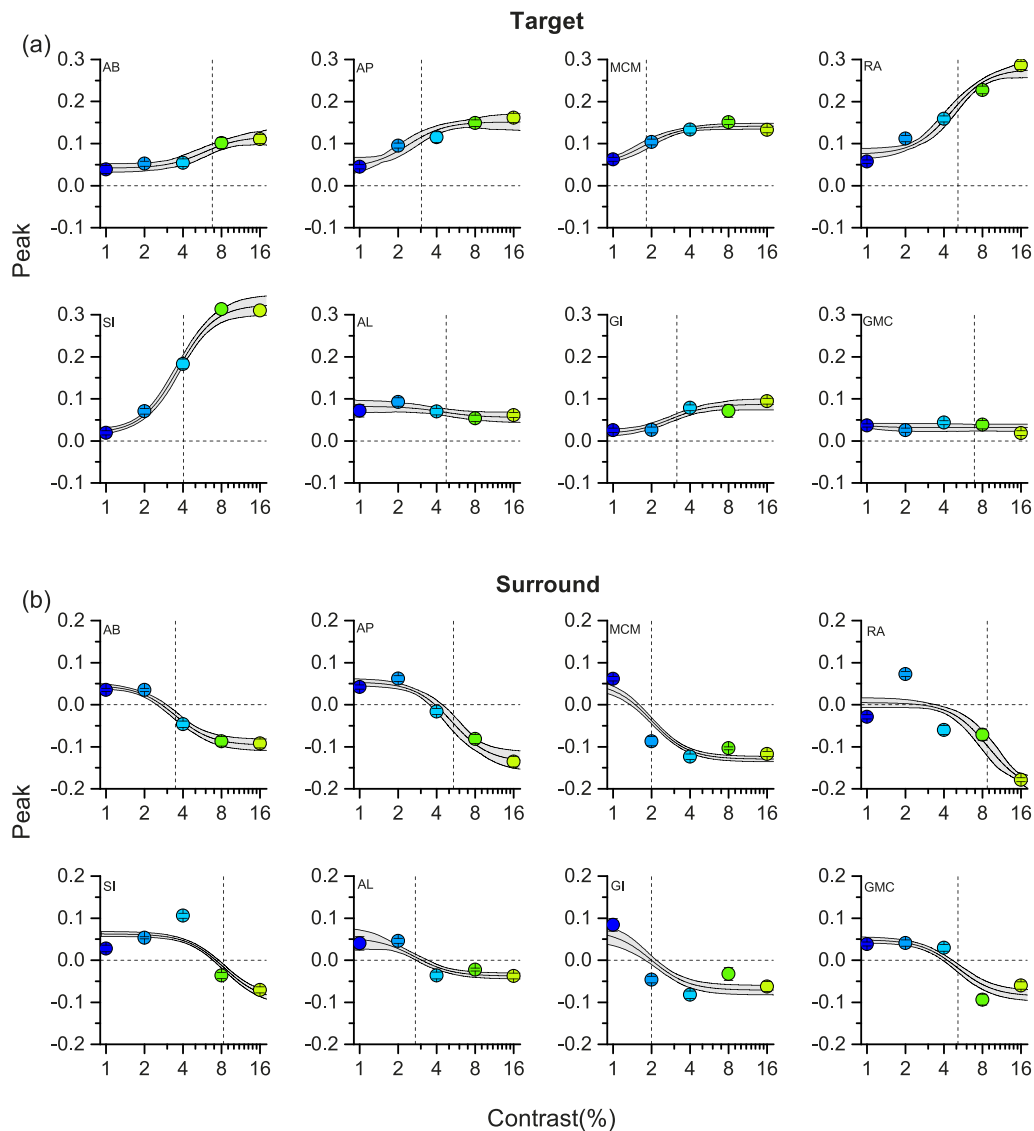
Figure 8. Peak amplitudes for the target and the surround kernels as a function of contrast, for eight observers. The cross-correlograms between response and target are plotted in (a), and those between response and surround are plotted in (b). Continuous lines show best-fitting Naka–Rushton function along with 95% confidence bands; dashed vertical lines indicate C_{50} values. To reduce degrees of freedom, β was fixed to 3 (see Supplementary File S2 for all the fit parameters).

Discussion

In this study, we adapted a recently developed technique of position tracking to make continuous psychophysical judgments about direction of motion, and replicated several well-known psychophysical effects (Bonnen et al., 2015a). In particular, the technique was able to replicate poorer motion perception at higher spatial frequencies (8 vs. 1 c/°) and the monotonic relationship between tracking and stimulus contrast, following the compressive Naka–Rushton law (Naka & Rushton, 1966). Importantly, we used the technique to study interactions between target regions and their surround. Again, expanding on traditional

psychophysics, we demonstrated antagonism between center and surround and showed that the antagonism occurs only at high contrasts; at low contrasts, the surround sums with rather than inhibits the center (Tadin et al., 2003).

Overall our work underlines several strong points of this approach. The first is that the technique is intrinsically capable of simultaneously measuring many effects, as the response can be correlated with the temporal evolution of several variables—in this case, with the independent motions of center and surround. It was very effective in demonstrating flanker effects on the target, even when subjects were instructed to ignore the flankers. The other main advantage of the technique is that it is quick, requiring only short
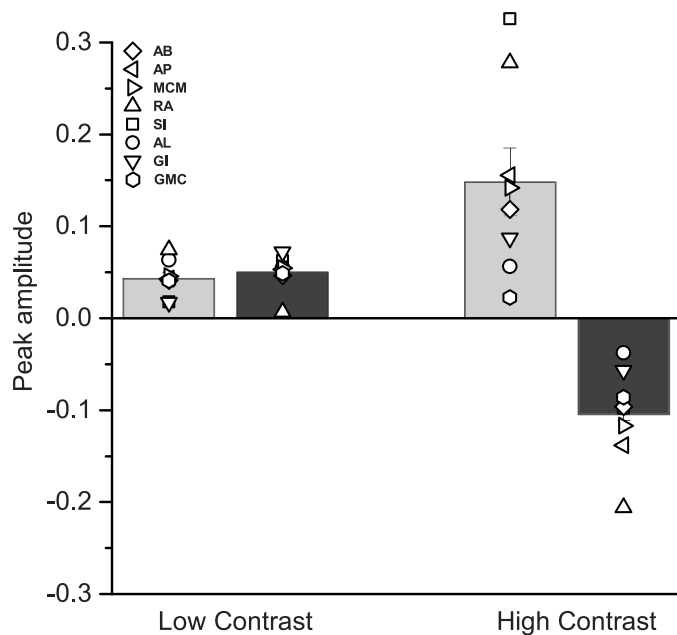
Figure 9. Kernel peaks for low and high contrast asymptotes of Naka–Rushton fits. Gray bars show the average response to the target, black bars to the surround; symbols show individual responses. Low contrast asymptotes are given by the baseline value (*B*) of the Naka–Rushton fit, and high contrast asymptotes by the sum of the amplitude and baseline (*A* and *B*) of the same fit.

sessions of data collection. The contrast-dependent surround effect was evident after only a very short session, lasting just 3 min.

Our work also revealed that performance varied somewhat across observers. Although this was not the primary aim of the current experiment, it strongly suggests that future studies need to follow a within-subject design.

At the same time, it is possible that with a few amendments our technique could become even more efficient and enjoyable. For instance, we employed a rather high rate of direction change (50% probability of reversal every 16 ms), which clearly exceeds the temporal resolution of the subjects' response capabilities. This rate was chosen to generate stimuli containing a near-flat spectrum, which yields the most accurate estimate of the response kernels. However, the kernels we measured have relatively long integration constants, suggesting that similar results could be obtained even with less frequent direction changes, with the added benefit of a less taxing experimental demand. Confining the frequency range of our stimulus to that most useful for the task would be similar to the techniques used in reverse correlation, where particular features rather than pure white noise can be used to optimize data collection (Murray, Bennett, & Sekuler, 2002).

We found that for the conditions we examined (spatial frequency and contrast), only the peak of the correlogram varies in a systematic way: The other two candidate parameters, lag and width, seemed to be largely uninformative. This differs from the study by Bonnen et al. (2015), who showed that all three parameters varied in a predictable way with stimulus salience. It is far from clear why this difference arose. One possibility is that the two tracking tasks were different: Where observers for Bonnen et al. had to continually track the exact position of a target in two dimensions, our observers indicated the instantaneous direction of motion with a binary decision, left or right. This simpler response may not lead to changes in the lag and width of the correlogram.

Our results are broadly consistent with those of Tadin and colleagues (Tadin et al., 2003; Tadin, 2006), who examined the effects of size and contrast on motion perception by looking at duration thresholds as a dependent variable. They found that at low contrasts (2.8%), duration thresholds decreased with increasing size, reaching a lower asymptote at about 40 ms. For all other contrasts (from 5.5% to 92%), duration thresholds increased systematically with increasing size (Tadin et al., 2003). In Figure 8 we demonstrate similar effects of contrast, keeping the size of the stimuli constant. At lower contrasts, peak values of the surround are positive, suggesting spatial pooling or summation. The peaks grow farther apart for the same-size target after 4% contrast, suggesting active surround suppression at higher contrasts. It is interesting to compare the overall experimental duration of our experiment to that of Tadin (2006), which employed reverse correlation. In that experiment each curve was derived from 2,500 trials requiring about 2 hr of data collection. In our experiment each condition required about 5 min of data collection including rest, indicating a clear advantage of our technique.

The results are also consistent with neurophysiological evidence from recording neuronal responses to stimuli of different sizes and contrasts in macaque MT. Surround suppression in MT neurons is highly contrast dependent (Tsui & Pack, 2011).

The surround antagonism clearly relates to the well-known phenomenon of induced motion, commonly illustrated by the fact that when large moving clouds pass the moon, the moon appears to sail past stationary clouds. Duncker (1929) quantified the effect, showing that a target moving downward past leftward-moving stimuli appears to drift down to the left (see also Anstis & Casco, 2006). Loomis and Nakayama (1973) pointed out that this type of motion contrast most likely relies on surround-inhibition mechanisms. Our tracking results provide strong evidence that surround inhibition is probably behind the induced-motion illusion, in that

it follows the contrast dependence observed both psychophysically (Tadin et al., 2003) and physiologically (Tsui & Pack, 2011) for motion surround-inhibition. It also provides a technique to directly quantify the effect of the surround on the central target.

Keywords: motion perception, surround antagonism, continuous psychophysics

Acknowledgments

Commercial relationships: none.
Corresponding author: David C. Burr.
Email: davidcharles.burr@unifi.it.
Address: Department of Neuroscience, University of Florence, Florence, Italy.

References

Ahumada, A. J. (1996). Perceptual classification images from vernier acuity masked by noise. *Perception*, 26, 18, https://doi.org/10.1068/v96l0501.

Allman, J., Miezin, F., & McGuinness, E. (1985). Direction- and velocity-specific responses from beyond the classical receptive field in the middle temporal visual area (MT). *Perception*, 14(2), 105–126, https://doi.org/10.1068/p140105.

Anobile, G., Castaldi, E., Turi, M., Tinelli, F., & Burr, D. C. (2016). Numerosity but not texture-density discrimination correlates with math ability in children. *Developmental Psychology*, 52(8), 1206–1216, https://doi.org/10.1037/dev0000155.

Anstis, S., & Casco, C. (2006). Induced movement: The flying bluebottle illusion. *Journal of Vision*, 6(10):8, 1087–1092, https://doi.org/10.1167/6.10.8. [PubMed] [Article]

Barlow, H. B. (1981). Critical limiting factors in the design of the eye and visual cortex. *Proceedings of the Royal Society B*, 212, 1–34, https://doi.org/10.1098/rspb.1981.0022.

Bonnen, K., Burge, J., Yates, J., Pillow, J., & Cormack, L. K. (2015). Continuous psychophysics: Target-tracking to measure visual sensitivity. *Journal of Vision*, 15(3):14, 1–16, https://doi.org/10.1167/15.3.14. [PubMed] [Article]

Brainard, D. H. (1997). The Psychophysics Toolbox. *Spatial Vision*, 10(4), 433–436, https://doi.org/10.1163/156856897X00357.

Chubb, C., Sperling, G., & Solomon, J. A. (1989). Texture interactions determine perceived contrast. *Proceedings of the National Academy of Sciences, USA*, 86, 9631–9635, https://doi.org/10.1017/CBO9781107415324.004.

Churan, J., Khawaja, F. A., Tsui, J. M. G., & Pack, C. C. (2008). Brief motion stimuli preferentially activate surround-suppressed neurons in macaque visual area MT. *Current Biology*, 18, 1051–1052, https://doi.org/10.1016/j.cub.2008.10.003.

Duncker, K. (1929). Über induzierte Bewegung—Ein Beitrag zur Theorie optisch wahrgenommener Bewegung. *Psychologische Forschung*, 12(1), 180–259, https://doi.org/10.1007/BF02409210.

Hartline, H. K. (1940). The receptive fields of optic nerve fibers. *American Journal of Physiology*, 130, 690–699.

Kleiner, M., Brainard, D. H., Pelli, D. G., Broussard, C., Wolf, T., & Niehorster, D. (2007). What's new in Psychtoolbox-3? *Perception*, 36, https://doi.org/10.1068/v070821.

Loomis, J. M., & Nakayama, K. (1973). A velocity analogue of brightness contrast. *Perception*, 2(4), 425–428, https://doi.org/10.1068/p020425.

Mulligan, J. B., Stevenson, S. B., & Cormack, L. K. (2013). Reflexive and voluntary control of smooth eye movements. *SPIE*, 8651, 1–22, https://doi.org/10.1117/12.2010333.

Murray, R. F., Bennett, P. J., & Sekuler, A. B. (2002). Optimal methods for calculating classification images: Weighted sums. *Journal of Vision*, 2(1):6, 79–104, https://doi.org/10.1167/2.1.6. [PubMed] [Article]

Naka, K. I., & Rushton, W. A. H. (1966). S-potentials from luminosity units in the retina of fish (Cyprinidae). *The Journal of Physiology*, 185(3), 587–599, https://doi.org/10.1113/jphysiol.1966.sp008003.

Neri, P., & Levi, D. M. (2006). Receptive versus perceptive fields from the reverse-correlation viewpoint. *Vision Research*, 46, 2465–2474, https://doi.org/10.1016/j.visres.2006.02.002.

Tadin, D. (2006). Fine temporal properties of center-surround interactions in motion revealed by reverse correlation. *The Journal of Neuroscience*, 26(10), 2614–2622, https://doi.org/10.1523/JNEUROSCI.4253-05.2006.

Tadin, D., Lappin, J. S., Gilroy, L. A., & Blake, R.

(2003, July 17). Perceptual consequences of centre–surround antagonism in visual motion processing. *Nature*, *424*(6946), 312–315, https://doi.org/10.1038/nature01812.1.

Tsui, J. M. G., & Pack, C. C. (2011). Contrast sensitivity of MT receptive field centers and surrounds. *Journal of Neurophysiology*, *106*(4), 1888–1900, https://doi.org/10.1152/jn.00165.2011.

Wiesel, T. N., & Hubel, D. H. (1965). Extent of recovery from the effects of visual deprivation in kittens. *Journal of Neurophysiology*, *28*(6), 1060–1072, https://doi.org/10.1152/jn.1965.28.6.1060.